Preprints (www.preprints.org) | NOT PEER-REVIEWED | Posted: 9 November 2021 doi:10.20944/preprints202105.0496.v2

An Explanation and Understanding of Aerodynamic Lift by Triple-Deck Theory *

A.P. Schaffarczyk
Kiel University of Applied Sciences
Alois.Schaffarczyk@FH-Kiel.de

November 9, 2021

Abstract

An explanation of aerodynamic lift still is under controversial discussion as can be seen, for example, in a recent published article in Scientific American [1]. In contrast to the use of integral conservation laws we here review an approach via the classical Kutta-Condition and its relation to boundary layer theory. Thereby we summarize known results for viscous correction to the lift coefficient for thin aerodynamic profiles and try to remember the work on Triple-Deck Theory (TDT) or higher order Boundary Layer theory. Connection to interactive boundary layer theory, viscous/inviscid coupling as implemented to well-known engineering code Xfoil is discussed. Finally we compare findings from tDT with 2D numerical solutions of full Navier-Stokes equations (CFD)models. As a conclusion, a clearer definition of terms like understanding and explanation applied to the phenomenon of aerodynamic lift will be given.

Keywords: Aerodynamic Lift, Kutta-Joukovsky-Condition, Interactive Boundary Layer Theory, Triple-Deck-Theory

*This manuscript was submitted to mdpi *fluids* but rejected for publication. An updated version includes changes due to critique and recommendations by the reviewers.

 doi:10.20944/preprints202105.0496.v2

Contents

List of Figures

Preprints (www.preprints.org) | NOT PEER-REVIEWED | Posted: 9 November 2021 doi:10.20944/preprints202105.0496.v2

Preprints (www.preprints.org) | NOT PEER-REVIEWED | Posted: 9 November 2021 doi:10.20944/preprints202105.0496.v2

1 Introduction: Definition of an explanation

Since the emergence of *Quantum Physics*, an understanding of certain phenomena like quantum mechanical superposition is highly non-trivial. Fortunately, Fluid Mechanics is what is termed **Classical Mechanics** and may be related to every-day experiences and is thus much easier to explain than quantum mechanical phenomena.

However, sometimes it seems that a discussion around aerodynamic lift is closer to quantum mechanics than to classical mechanics which may be related to the fact, that the mathematical description is *classical* but in terms of a non-linear field-theory.

Here we take the following point of view:

1. We have a theory (or model) for some phenomena if we have a set of assumptions resulting in equations for quantitative descriptions to be compared with measurements.

2. Pure numerical solutions from the most basic equations are not sufficient as they only produce very specific results.

To remind to the basic concepts of Mechanics we may start by shortly referring to Newton's 2^{nd} law for a point mass:

$$F = \dot{p} \; . \tag{1}$$

A force (in N) relates to the temporal change of momentum $p = m \cdot v$. A *cause and effect* relationship may be established in **both** directions, meaning that a force is a cause for a change in momentum, or a change in momentum may be the cause for an inertial force.

Fluid mechanics as a continuum theory is formulated in terms of a velocity *field* $\mathbf{v}$ and expresses momentum change (mChange) and mass conservation (mCons):

$$\text{mChange:}\; \rho\left(\frac{\partial \mathbf{v}}{\partial t} + (\mathbf{v}\cdot\nabla)\mathbf{v}\right) = \mathbf{f} - \nabla p + \mu\Delta\mathbf{v} \; , \tag{2}$$

$$\text{mCons:}\; \nabla\cdot\mathbf{v} = 0 \; . \tag{3}$$

Here, and in the following we assume *incompressible* and *sub-sonic* flow. Instead of the quantity *force* it introduces a *static pressure p* and a *volume force density f* (N/m^3). To calculate a force on an extended body (airfoils) one has to integrate pressure (and viscous shear stress) on its surface. However, the relation of the local pressure to the velocity is non-local, as can be seen from the following derivation: By use of Eq. (3) pressure can be eliminated but then the dependency of pressure on velocity becomes *non-local*:

$$\text{From } \Delta p = -\rho \frac{\partial^2 u_i u_j}{\partial x_i \partial x_j} := S(\mathbf{r}) \; , \tag{4}$$

 doi:10.20944/preprints202105.0496.v2

this equation may then be solved by the introduction of *Green's function*:

$$p(\mathbf{r}) = p^{harmonic}(\mathbf{r}) + p(\mathbf{r}) + \frac{\rho}{4\pi}\int_{\mathbb{R}^3} \frac{S(\mathbf{r})}{|\mathbf{r}-\mathbf{r}'|}\, d\mathbf{r}' \;, \tag{5}$$

where $p^{harmonic}(\mathbf{r})$ is a solution of the homogeneous pressure equation:

$$\Delta p^{harmonic}(\mathbf{r}) = 0 \;. \tag{6}$$

We will come back to this in connection with formulating boundary conditions for the pressure at the TE, se Eq (53) Contrarily to p $\mathbf{f}$, the body-force density usually is regarded as given from *outside* and in many cases does not have to be included. (With an exception of the so-called Actuator Disk see [6].)

In the rest of the paper we proceed as follows: We review basic models of lift in a more logical manner than they appeared historically, compare them with numerical simulations and conclude with a physical model which in our understanding provides a (long known) explanation of aerodynamic lift. An appendix finally provides more technical details of the Triple-Deck-Theory.

We have to remark that our review mainly follows an approach in the spirit of Landau [7] which from the beginning emphasis the role of a wake emerging down stream of an aerodynamic profile.

Therefore it is rather different from that of McLean [5, 8, 9] who emphasizes the non-local pressure field *as a direct result of the lift force* [9] and its *reciprocal* interaction with the velocity field as a key ingredient of a qualitative explanation of lift and not as pessimistic as expressed in an already mentioned article by Regis [1].

2 Thin Airfoil Theory

2.1 A First Encounter with History of Explanations of Aerodynamic Lift

Specific shaped 2D sections exhibit a large force perpendicular to the inflow direction. This force is called lift. It may be defined as the projection of static pressure (inviscid case, direction given by local surface normal) and shear stress (viscous flow, direction tangential to surface).

Nowadays, not only airplanes use it but also most of the highly efficient machines, e.g. helicopters, ship propellers and wind turbines. Nevertheless, even today, there is a discussion [5] for an explanation (in the sense of a cause and effect relation mentioned above) as it was in the beginning of the 20th century. Bloor [10] gives an excellent and very readable review of some of the early historical developments from about 1900 to 1930. In short two *schools* used either Newton's corpuscular picture or the newly emerged circulation model.

2.2 Inviscid Thin Airfoil theory

A first important step in developing a theory of aerodynamic lift, of what one may term even an understanding was the formulation of the so-called Kutta-

Preprints (www.preprints.org) | NOT PEER-REVIEWED | Posted: 9 November 2021 doi:10.20944/preprints202105.0496.v2

Joukovsky theorem [11] which states

$$L = -\rho \cdot w \cdot \Gamma \ . \tag{7}$$

Here L is the lift force (per unit span), ρ the density of the fluid, w the inflow velocity (far up-stream) and Γ the circulation, defined as

$$\Gamma := \oint_C v \cdot dr \ . \tag{8}$$

C is an arbitrary closed loop around the airfoil.

Therefore, a dynamical quantity (lift) is connected to fully kinematic quantities (w, Γ), only. Sign conventions are as follows:

1. velocity: left to right,
2. lift: from bottom to top,
3. circulation: counter-clockwise.

This explains the negative sign in Eq. (7).

A unique circulation, needed for a unique defined lift, needs a formulation of additional assumptions and this resulted in the so-called Kutta-condition. It may be stated in various forms. If the airfoil tail (x/c = 1) is regarded to have a non-smooth change in geometrical slope from the upper to the lower side (known as the trailing edge), it is usually expressed - as a more mathematical statement - demanding that all velocities at the trailing edge should be finite, i.e. $< \infty$. Note that inviscid potential theory does not forbid infinite velocities.

For an ellipse there is no sharp TE, therefore a severe logical loop-hole exists at least for these kind of trailing edges. However, Howarth as early as 1935 [12] managed to calculate lift and drag manually for this particular shape, an ellipse, by what is now called interactive boundary layer theory and its expression is found in the well-known code XFOIL [13]. Sears [14] took these ideas further and formulated corresponding conditions for static pressure at the upper and lower edges of the boundary layers in the sense of generalizing the Kutta-Joukovsky condition to viscous (boundary layer) flow.

The complete transient procedure on how circulation is generated from rest is still under investigation, see for example [15, 16] for a recent work.

Thin airfoil theory (TAT, called that way because any influence of the finite thickness of an airfoil is neglected) [17] gives a remarkable simple expression for the lift-coefficient

$$c_l = 2\pi \cdot (\alpha + \alpha_0) \ . \tag{9}$$

A lift-curve slope of 2π - independent of all geometrical details - therefore is predicted and the angle-of-attack (AOA) appears to be the most important quantity. Nevertheless, one particular geometrical quantity, camber (f), enters Eq 9 via $\alpha_0 = 2f$ shifting zero-lift AOA to negative angles. If flow direction is counted positive as when coming from the left, a positive AOA is given when the airfoil is rotated in clock-wise direction.

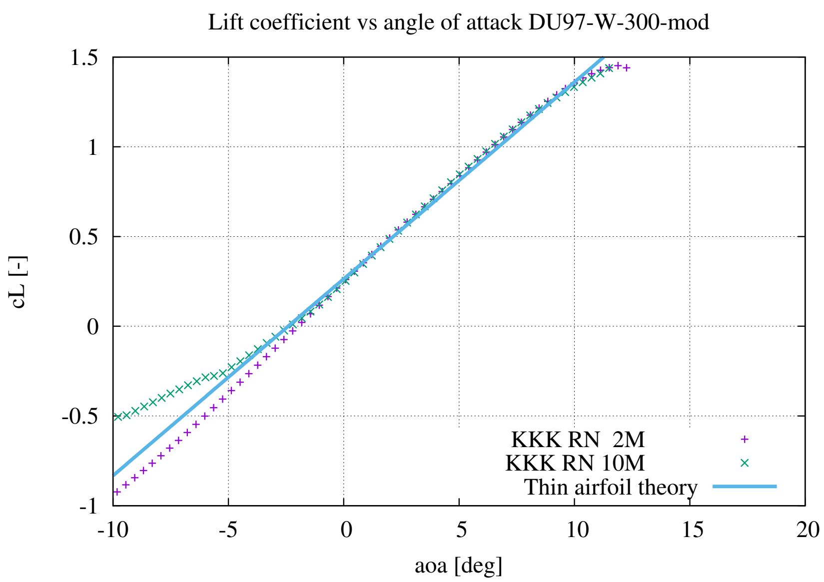

Figure 1: Comparison of measured lift coefficient vs angle-of-attack with thin airfoil theory showing a large region of linear variation until close to c_L^{max}. Results for RN 2 and 10 million are shown. For RN of 10 M separation on the lower (pressure) side occurs much earlier than for RN of 2 M.

Fig 1 compares measurements [18] of a 30% thick airfoil - with 2.1 % camber - dedicated for wind turbine blades with prediction of thin-airfoil-theory. A remarkably large (more than 20 degrees) range of agreement (within the experimental uncertainty) even for this certainly not-thin airfoil exists.

2.3 Viscous Thin Airfoil Theory I: $RN << 1$

TAT is based on inviscid models of fluid flows (only density as a material enters) and as a consequence, e.g. circulation is a conserved quantity, i.e. it can neither be created nor destroyed. Therefore, more sophisticated models (and equations) must be included if the emergence of lift is to be explained. It is well known that the Navier-Stokes Equations provide this basis, adding a second material parameter, viscosity. In a series of journal and technical papers Yates [19] (and independently Bryant and Williams [20] and Shen and Crimi [21]) with the help of a Oseen-type approximation (in fact a linerization) were able to use these Navier-Stokes equations to

1. derive and thereby explain the Kutta condition and
2. to give asymptotic corrections to the lift-curve slope in terms of inverse Reynolds number.

This is somewhat surprising as Oseen-Flow, see [11], chapter (4.10), is generally assumed to be valid in low-Re (RN<1, creeping) flow only, whereas in high-Re flow (RN $> 10^5$) boundary layer theory [22] should be more appropriate. As a consequence numerical agreement for changes in the lift-slope (with reference to $2 \cdot \pi$) were not convincing. Liu et al. [23] investigates the influence of viscosity to the generation of lift at small RN (=200). Her findings indicate that a non-linear $c_L(\alpha)$ curve should be more approprate in contrast to a linear one from Yates' model but with modified slope only [24].

2.4 Aerodynamic Profiles with Finite Thickness

In this context, to separate between *thickness* and *viscous* effects a lot of authors including Abbot and von Doenhoeff [25] tried to improve (inviscid) TAT by investigating the influence of thickness on the lift-curve-slope which typically results in equations like: [25],

$$c_L = 2\pi\,(1+\tau)\,\alpha\;, \tag{10}$$

$$\tau = \frac{\epsilon}{a} = \frac{4\sqrt{3}}{9}\cdot\frac{t}{c}\;. \tag{11}$$

Yates [26, 24] combined Reynolds number and thickness corrections to

$$c_L = 2\pi\,(1+\tau)\cdot\left(1-\frac{4}{\log\left(64RN\right)+\gamma_E}\right)\cdot\alpha \tag{12}$$

$\gamma_E = 0.57722$ being Euler's constant which shows a decrease of more than 10 % at t/c = 0.3 and RN around 10^5 from RN effects which - at least - is partly

Preprints (www.preprints.org) | NOT PEER-REVIEWED | Posted: 9 November 2021 doi:10.20944/preprints202105.0496.v2

compensated by the first (thickness) term. McLean [5], chapter 7.4, pp 313/314 gives further details.

Not included in all these discussions is the influence of the flow-state of the boundary layer, whether it is laminar or turbulent. In our discussions we assume that lift (in the linear part) is not influenced as strongly as drag. It is well known that drag can be much higher when most parts of the boundary layer are turbulent.

Another important phenomenon, flow separation, the starting point defined by

$$\tau_W = \mu \cdot \frac{dv_t}{dn} \leq 0 \,. \tag{13}$$

Separation usually limits c_L (as measured) to values from 1.0 to about 2.0. We will come back to that in section 4.5 as there is a close inter-dependency between separation and some TAT scales .

We implicitly assume that the effect of separation can be approximately described by shifting the trailing edge to the points of separation [12, 14]. This restricts our discussion to small AOA only ($-1^\circ < \alpha < 5^\circ$).

3 Viscous correction to Lift Coefficient by Schmitz

Schmitz [27, 28, 29] calculated finite domain viscous correction and found small deviations (10^{-2} of inviscid circulation) only for an airfoil flow at Re = 500 k [20]. As a result a typical reduction in c_L of

$$\Delta c_L =\sim -2\left(\frac{U_e}{U_\infty}\right)^2\left(\frac{\delta_{TE}}{c}\right)^2 \,, \tag{14}$$

is predicted. Here, U_e resp. U_∞ is the velocity at the edge of the boundary layer at the trailing edge (TE) resp. the inflow velocity; δ_{TE} is the boundary layer thickness and c the chord of the profile. A simple estimation for RN $\sim 10^6$ shows that the resulting reduction depends on the type of the flow and is comparable small for a pure laminar boundary layer. It is interesting to note that Triple-Deck Theory (see section 4.5) is able to derive a similar (but with more explicit RN-dependendy) expression which reads as [30]

$$\frac{3}{8\pi c}\left(\delta_1 + \theta\right) RN^{-1/2} \cdot \log\left(RN\right) . \tag{15}$$

Here δ_1 and θ is the displacement thickness and momentum thickness at the trailing edge, resp.

4 Viscous Thin Airfoil Theory II: $RN >> 1$

4.1 Boundary Layer Theory

Boundary layer theory (BLT) was initiated by the seminal paper of Prandtl [31]. As one of the first applications a semi-infinite flat plate located at $x > 0$ and y =

Preprints (www.preprints.org) | NOT PEER-REVIEWED | Posted: 9 November 2021 doi:10.20944/preprints202105.0496.v2

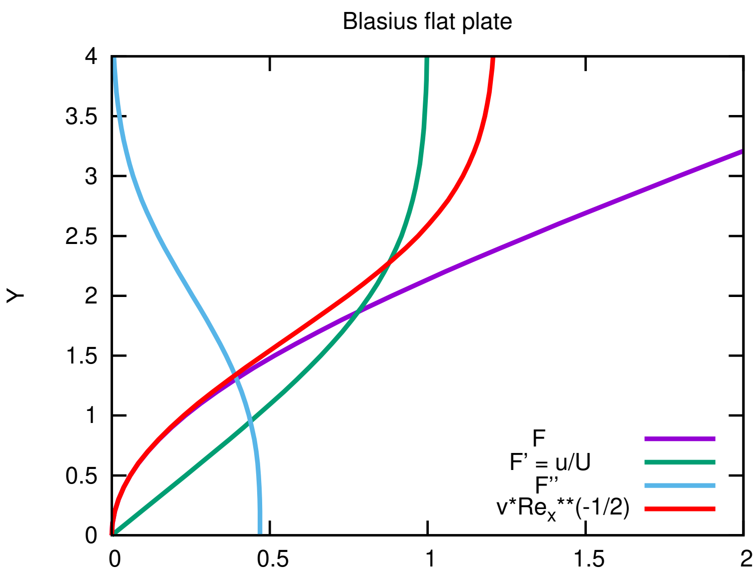

Figure 2: Stream function (F) and velocity profile (F') from numerical Integration of Eq. (16). F"(y=0) correspond to wall shear stress. In addition, it can be seen that the normal velocity v approaches a finite value $\sim \sqrt{RN_x}$ when the boundary layer edge is reached.

0 was investigated by Blasius [32]. Using a similarity transformation he reduced the Navier-Stokes Equations to a still non-linear but much simpler ordinary differential equation for an auxiliary function F with the stream function being $\sqrt{2x}F$:

$$F''' + F \cdot F'' = 0 \; , \tag{16}$$

together with boundary conditions $F(0) = F'(0) = 0$ and $F(s) \to s$ as $s \to \infty$. Here $s = Y/\sqrt{2x}$, with x the non-dimensionalized coordinate in flow direction, Y the inner coordinate normal to the plate and scaled with $\delta_0(RN)$ the length scale of the boundary layer.

Blasius was able to represent the solution as a power series (see [33, 34, 35] for mathematical details)

$$F(s) = \frac{1}{2}\lambda s^2 - \frac{1}{240}\lambda^2 s^5 + \frac{11}{161280}\lambda^3 s^8 + ... \tag{17}$$

$$\text{with: } \lambda = F''(y = 0). \tag{18}$$

With $Re_x = u_\infty \cdot x/\nu$ it follows

$$\delta_{99} = 5.0 \cdot Re_x^{-1/2} \;\; \text{at y where } u = 0.99 \cdot U_\infty \; , \tag{19}$$

$$\delta_1 = 1.72 \cdot Re_x^{-1/2} \;\; \text{displacement thickness} \; . \tag{20}$$

It must be noted, that today Eq. (16) is typically solved numerically to arbitrary accuracy, see Fig 2. The asymptotic behavior $y \to \infty$ can be studied by assuming

$$F(y) = y - \beta_0 + g_o(y) \; . \tag{21}$$

It follows [2]

$$\beta_0 = 1.21649 \; , \tag{22}$$

$$g_0(y) = exp(-\frac{y^2}{2}) \; . \tag{23}$$

Fig. 3 shows the accuracy of both Taylor series around 0 and ∞.

4.2 Drag, Comparison with Experiment and Higher Order Boundary Layer Theory

As wall shear stress is related to $F''(y \to 0)$ drag can then be calculated by integration and further compared to measurements. Two findings are important:

1. for $Re_x > 5 \cdot 10^5$ flow state starts changing to a turbulent one,

2. for $Re_x < 10^4$ deviations become larger as expected, see Fig 4.

Improvement is possible if BLT is regarded as an asymptotic expansion in powers of inverse Reynolds number. First order then are terms $\sim RN^{-1/2}$. As one can see from the dashed line in Fig 4, there is significant improvement - even down to $Re_x \sim 10$ - if one takes higher orders into account as will be seen in section 4.5.

Preprints (www.preprints.org) | NOT PEER-REVIEWED | Posted: 9 November 2021 doi:10.20944/preprints202105.0496.v2

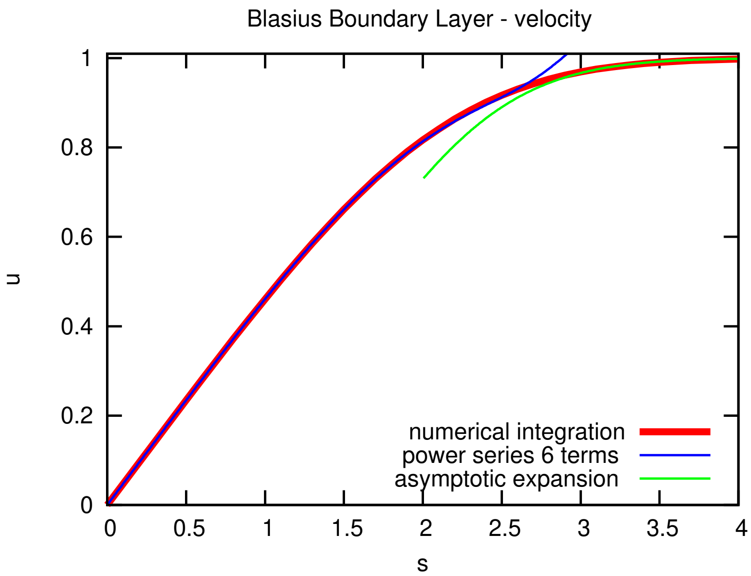

Figure 3: F' (velocity profile) and its representation by a 6-term power series and asymptotic expansion. The rather large (more than 14 digits) integer coefficient were calculated with the help of MATHEMATICA ©.

However, it has to be added, that McLachlan [36] showed that this is mainly due to a fortunate cancellation of terms $\sim RN^{-1}$,

Blasius (solid line):

$$c_D = 2 \cdot 0.665146724 \cdot (Re)^{-1/2} \tag{24}$$

Triple-Deck-Theory (dashed line):

$$c_D = 2 \cdot 0.664 \cdot (Re)^{-1/2} + 2.67 \cdot (Re)^{-7/8} \tag{25}$$

Value for Re = 10:

$$c_D = 0.42 + 0.36 = 0.78 \ , \tag{26}$$

Value for Re = 1000:

$$c_D = 0.042 + 0.006 = 0.048 \ . \tag{27}$$

Eq. (25) contains a new term $\sim Re^{-7/8}$ (note that the exponent is not **-1** but **-7/8**) which contributes to more than 10 % to the drag and which will be discussed in more detail below.

4.3 Flat plate of finite length

Having described the problem of a semi-infinite plate ($x > 0$) we turn to a flat plate of **finite** length: $-1 < x < 0$, still aligned to the inflow:

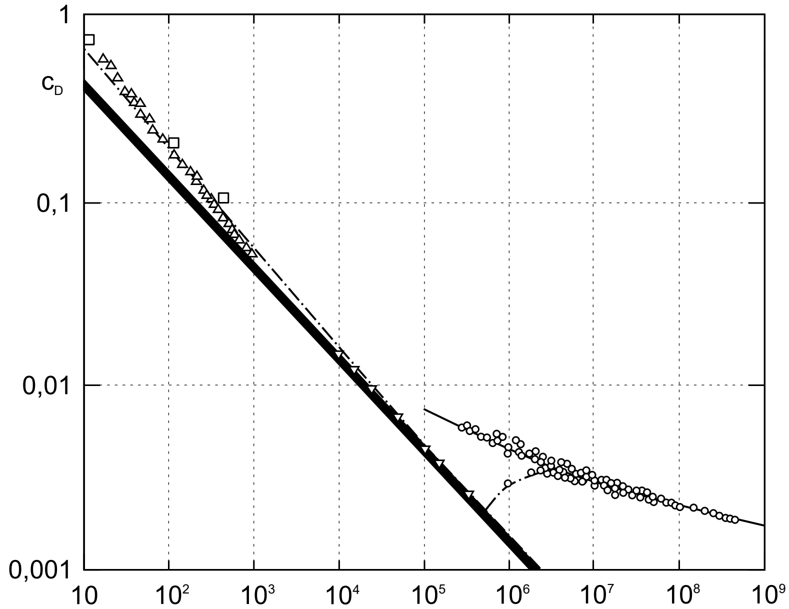

Figure 4: Comparison of drag coefficient from BLT and measurements. Fat line: Blasius, dashed line: higher order (Triple-Deck) and empirical correlation for the turbulent case. x-axis: RN, y-axis: c_D

Preprints (www.preprints.org) | NOT PEER-REVIEWED | Posted: 9 November 2021 doi:10.20944/preprints202105.0496.v2

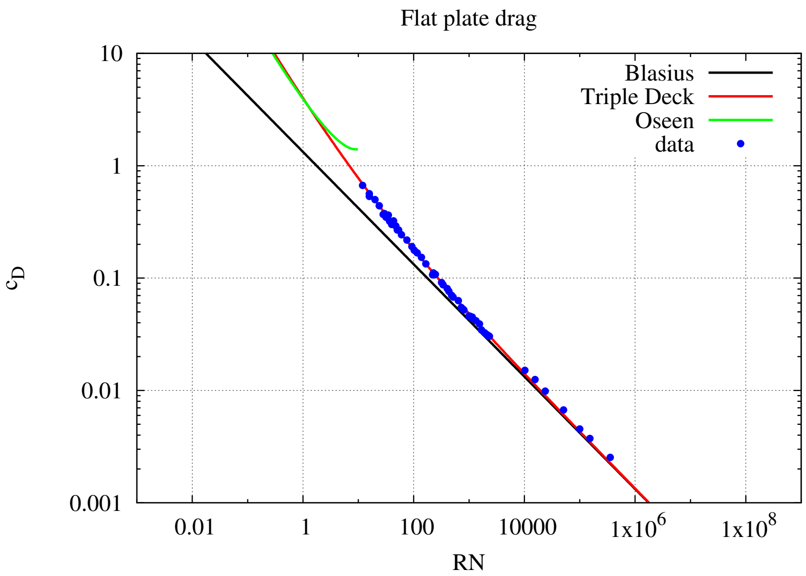

Figure 5: Drag coefficient of a flat plate in the laminar state and from various approaches: Measurements and Theories of Oseen, Blasius and the Triple-Deck-Theory for an extended RN region down to less than RN of 10^{-2}. Is it surprising that Oseen's low RN approximations even has an overlapping with TAT

4.4 Goldstein's inner and outer wake

Only some years later BLT was extended to a flat plate of finite length $-1 < x < 0, y = 0$ by Goldstein [37]. The situation is as follows: At the plate we have for y=0 u=0 which is simply the *no-slip condition*. Within the wake ($x > 0$) we will have $u \neq 0$. This different behavior at $y = 0$ for $x < 0$ and $x > 0$ is the reason, that the wake exhibits a two-fold structure, separated by a curve $y \sim x^{-1/3}$, see Fig. 6. Unfortunately, close to $x = 0$ a singularity appears:

$$v(x,0) \sim x^{-1/3}\,, x > 0\,, \tag{28}$$

which is named **Goldstein** singularity and can be calculated from $\Psi \sim x^{2/3}$ and $v \sim -\Psi_x$. It clearly violates the assumptions from BLT that $v \sim RN^{-1/2}$, see Fig. 2.

Although we will proceed with this approach we have to remark that Goldstein's model still is not sufficient for investigations on how the Kutta-Conditions emerges from viscous flows. Only if the flow velocity is at least continuous in all components we may be able to explain lift.

Analogously to Eq. (16) the wake is composed of **two** boundary layers (inner and outer wake) and therefore needs to be described in terms of two functions H_0, H_1 via:

$$3{H_0}''' + 2H_0{H_0}'' - {H_0'}^2 = 0\,, \tag{29}$$

$$3{H_1}''' + 2H_0{H_1}'' - 5{H_0}'{H_1}' + 5{H_0}''H_1 = 0\,. \tag{30}$$

Using $s = y/x^{1/3}$, it follows:

$$H_0 \sim \lambda_0^2 s + \frac{\lambda_0^4}{33!}s^3 - \frac{2\lambda_0^6}{95!}s^5\,, \tag{31}$$

$$H_1 \sim \lambda_1\lambda_0\left(s - -\frac{5}{18}\lambda_0^2 s^3\right) \text{ leading to} \tag{32}$$

$$u(x,0) \sim x^{1/3}\left(\lambda_0^2 + \lambda_0\lambda_1 x\right)\,. \tag{33}$$

Numerical integration leads to [2] $\lambda_0 = 0.8789, \lambda_1 = -0.1496$.

Fig. 6 displays the combined flat plate and wake boundary layers together with the governing equations. At the trailing edge $v \sim x^{-1/3}$ as $x \to 0^-$.

4.5 Triple-Deck Theory

The singularity close to $x = 0$ can only be removed by introducing a new, three fold structure with an extension in x $\sim RN^{-3/8} = RN^{1/8} \cdot RN^{-1/2}$, see Fig. 7. For example, for $RN = 10^5$, this corresponds to about 4 BL-thicknesses.

4.6 Flat plate at zero incidence

A considerable amount of work has to be done to remove the singularity mentioned above. First of all it is easy to show that the region close to the trailing

Preprints (www.preprints.org) | NOT PEER-REVIEWED | Posted: 9 November 2021 doi:10.20944/preprints202105.0496.v2

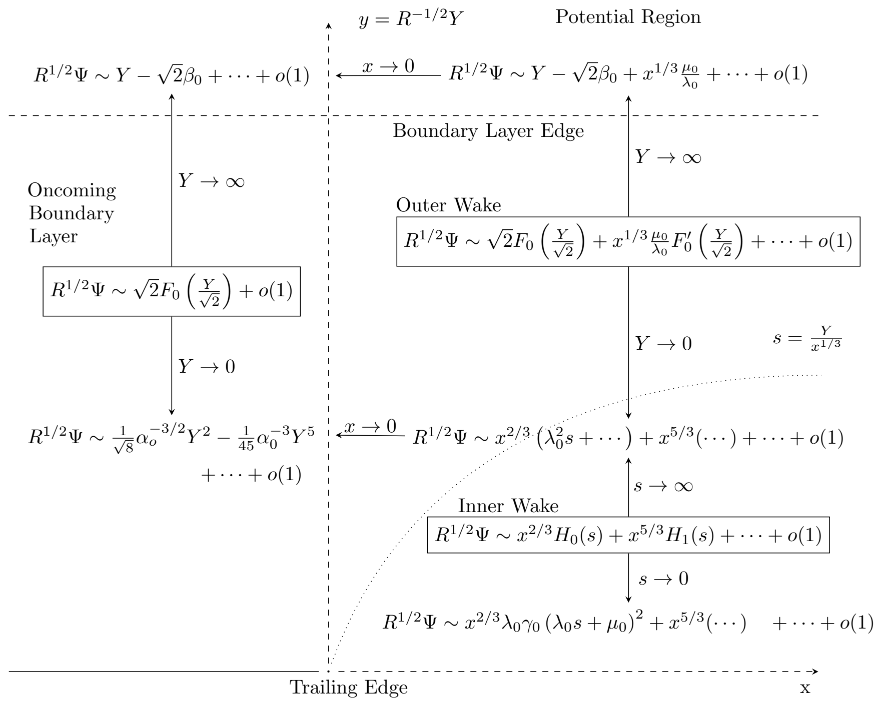

Figure 6: Goldstein's near wake structure. On the left Blasius boundary layer and on the right Goldstein's inner and outer wake. It clearly shows how the change in BoCos at the TE gives rise to the genesis of a new type (inner) wake. Nevertheless, the $x^{2/3}$ dependence (of the stream function) indicates emergence of singularities at the TE. Adapted from [2]
.

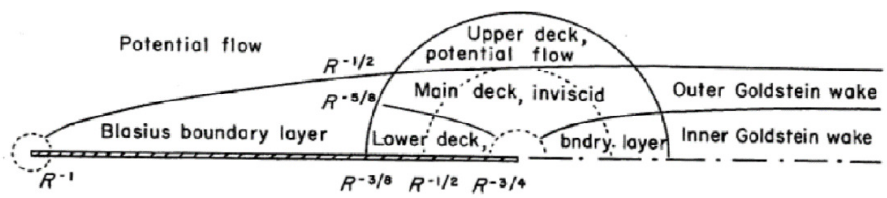

Figure 7: Modified Boundary Layer structure around the trailing edge of a flat plate. A region of extension $RN^{-3/8}$ around the trailing edge is divided into three layers or *decks from [3]*
.

Preprints (www.preprints.org) | NOT PEER-REVIEWED | Posted: 9 November 2021 doi:10.20944/preprints202105.0496.v2

edge - where BLT fails - scales according to $|x| \sim Re^{-3/8}$, see Sobey [2] or Sychev et al. [38].

Improving the properties of the analytical solution (in the sense of calculus) is now achieved by introducing the three-fold structure already mentioned above normal to the plate:

- Some kind of a *viscous sub layer*: the LOWER deck,
- A perturbation or interaction for the outer potential flow region, tranmitted in form of a displacement function $A_1(X)$: the OUTER deck,
- And in between the MIDDLE (or MAIN) deck, sometimes called *inviscid rotational disturbance* layer.

A sketch of the structure is visualized in Fig. 7.

Triple-Deck equations start with introducing appropriate scaled coordinates:

$$\text{Main deck: } Y = RN^{1/2}y \tag{34}$$

$$\text{Inner deck: } Z = RN^{1/8}Y \tag{35}$$

$$\text{Outer deck: } W = RN^{-1/8}Y \text{ and} \tag{36}$$

$$X = RN^{3/8}x\ . \tag{37}$$

$A_1(X)$ is defined via

$$\psi_1^m(X,Y) := A_1(X) \cdot U_0(Y) \tag{38}$$

and acts as a kind of a *displacement* function.

A characteristics set of equations can be derived [2]:

$$u_X + v_Z = 0 \text{ (mass conservation)} \tag{39}$$

$$uu_X + vu_Z = -\frac{1}{\pi}\int_{-\infty}^{\infty} \frac{A_1''(\zeta)}{X-\zeta} d\zeta + u_{ZZ}\ ; \tag{40}$$

together with asymptotics:

$$u \to \frac{\alpha_0^{-3/2}}{\sqrt{2}}[Z + A_1(X)] \text{ as } Z \to \infty, \tag{41}$$

$$A_1(X) \to 0 \text{ as } X \to -\infty, \tag{42}$$

$$A_1(X) \to \frac{\mu_0}{\lambda_0} X^{1/3} \text{ as } X \to \infty \text{ (inner part of the wake).} \tag{43}$$

In the appendices, see section (10) some more details of the mathematical properties of TDT are given. It has further to be noted that [39] in their appendix IV lists a 2nd-order TDT. This demonstrates that van Dyke's *matched asymptotic expansion* or as Cousteix and Mauss call it in an improved version *successive complementary expansion* can be regarded as a rational and reliable method. In addition, as early as 1996 [40] attempts have been made to formalize this approach by methods from *artificial intelligence*. Unfortunately, so far, no implementation in well-known systems like MATHEMATICA® has been published.

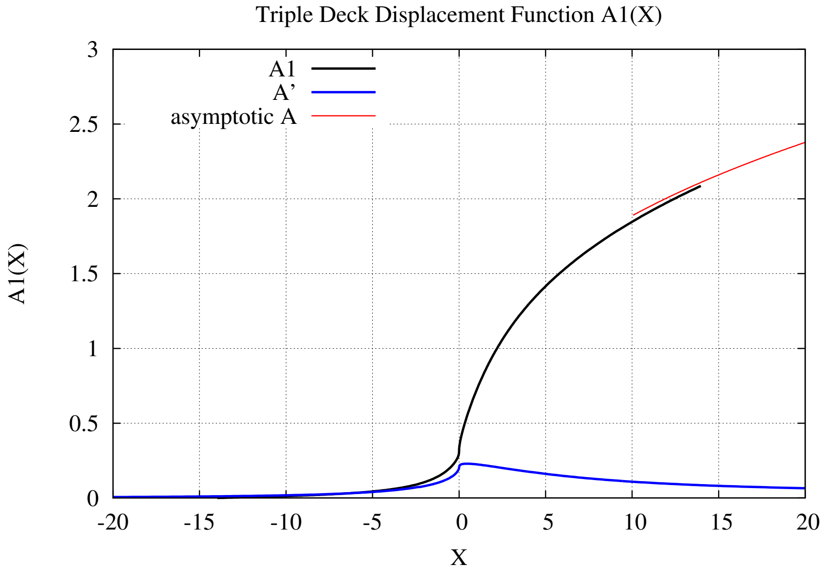

Figure 8: Triple-Deck displacement Function A_1 calculated with help of a FORTRAN code published by [2]. To scale A_1 in SI units it has to be multiplied by $RN^{-3/8}$. If RN=10^6 the scale then is $5.6 \cdot 10^{-3}$. A_1 must obey the asymptotic limit $\frac{\mu_0}{\lambda_0} X^{1/3}$ as $X \to \infty$ (red line). In addition $A_1{}'$ (which is proportional to the pressure) is included which is $\in \mathcal{C}^0$ (continuous) but $\notin \mathcal{C}^1$ (continuous differentiable).

Sobey [2] provides a set of FORTRAN routines for solving this non-linear set of integro-differential equations. Some sample results are presented in Fig. 8 and Fig. 9. As can be seen from the plots, all functions now are continuous at $x = 0$ (trailing edge) but still are not $\in \mathcal{C}^1$ (of continuous slope). For reasons of comparison we added results from CFD in Fig. 9.

Pressure is shown in Fig. 9 together with two asymptotics $p \sim$

$$-\frac{2}{3\sqrt{3}}\frac{\mu_0}{\lambda_0} RN^{-1/2}|x|^{-2/3} \; x < 0 \, , \tag{44}$$

$$\frac{1}{3\sqrt{3}}\frac{\mu_0}{\lambda_0} RN^{-1/2}x^{-2/3} \; x > 0 \, . \tag{45}$$

Singularity v $\to \infty$ at the trailing edge (see Eq. 28) disappears, because [41]

$$v \sim -A_1{}'(x) \, , \tag{46}$$

is finite for $X \to 0^{\pm}$. Unfortunately, streamlines close to the TE are not $\in \mathcal{C}^1$ (space of functions which are once continuous differentiable). Shifting this dis-continuity to even higher derivatives demands introduction of even more structure in form of more sub-layers [2, 38].

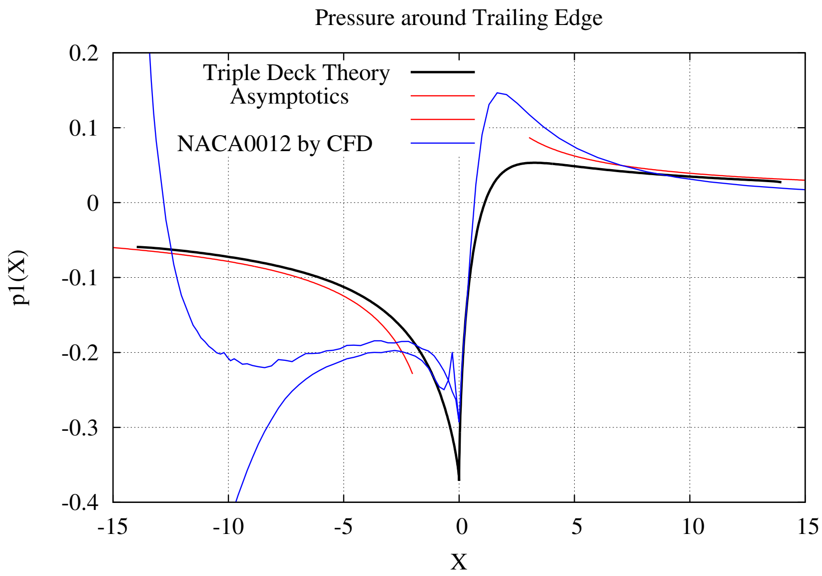

Figure 9: Pressure around trailing edge from Triple-Deck-theory [2] (black), together with asymptotic values from Blasius and Goldstein (red) and CFD for a thin airfoil (blue) see section 6. The two blue line upstream to the trailing edge correspond to the upper and lower side of the airfoil.

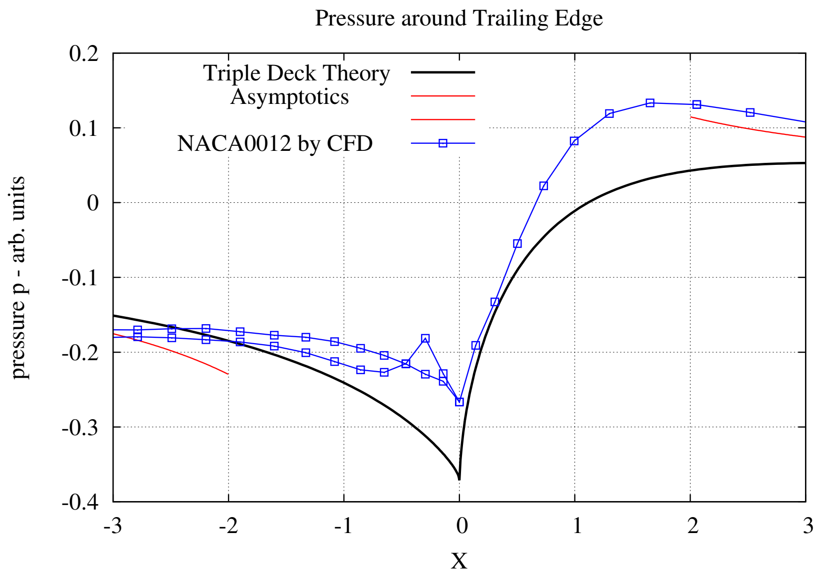

Figure 10: Same as Fig. 9, but enlarged. The apparently out-liner at $X \approx -0.3$ might be due to inaccurate geometric modeling of TE.

Nevertheless, one of the greatest success of TDT is an impressive improvement of prediction of finite length flat-plate drag coefficient. We will present these findings in more detail in section 6.

4.7 Flat Plate at an Incidence and Embedding of the Kutta Condition

The final step now is to apply the findings from section 4.5 to a flat plate of finite length and non-zero angle-of-attack which severs as a simple model of a 2D airfoil. This has been done already 50 years ago by Brown and Stewartson [42]. Summaries of up-dated derivations are given in [43] and [38] chapter 3.3 of. It is important to note that the *inviscid solution* is assumed to be

$$u = 1 - \alpha \frac{x + \Gamma}{(-x)\sqrt{(1+x)}} \cdot sgn(y)\ , v = 0 \quad (47)$$

$$\text{on the flat plate } y = 0, -1 < x < 0 \quad (48)$$

$$u = 1\ , v = \alpha \frac{x + \Gamma}{\sqrt{(x \cdot (1+x))}}\ y = 0, x > 0 \quad (49)$$

in accordance with the most general inviscid flow around a 2D body.

Apart from the *discontinuity* of the viscous boundary layer condition at the edge - a zero tangential velocity on the plate ($x \to 0^-$) faces a zero **pressure discontinuity** on the wake center-line ($x \to= 0^+$) - the phenomenon of separation determines the essential details of the flow close to the trailing edge.

To summarize, the following sequence of steps is necessary to derive the Kutta-Joukovsky-condition and a viscous correction to the lift coefficient for high Reynolds number flow:

Use outer potential flow consisting of an circulation part, (50)

Introduce triple deck length scale:

$$\epsilon = RN^{-1/8} = (U_\infty \cdot \ell/\nu)^{-1/8}\ . \quad (51)$$

TE separation excluded if AOA, $\alpha^\star = \epsilon^{1/2}\lambda^{9/8}\alpha < 0.47$. (52)

Demand unique pressure at Y=0 : $p_T(X) = p_B(X) < \infty, X \geq 0$. (53)

(54)

Eq. (53) may be regarded as some kind of a weaker *Kutta-Joukovsky-condition* but bearing in mind what was said in connection to Eq. (4) about the role of the pressure field

In total, this leads to:

$$\text{Lift coefficent: } c_L = 2\pi\alpha\left(1 - \frac{2B}{\ell}\right) \text{ with modified} \quad (55)$$

$$\text{Circulation term: } B = \epsilon^3 \ell \lambda^{-5/4} \cdot a_1 \quad (56)$$

(57)

Preprints (www.preprints.org) | NOT PEER-REVIEWED | Posted: 9 November 2021 doi:10.20944/preprints202105.0496.v2

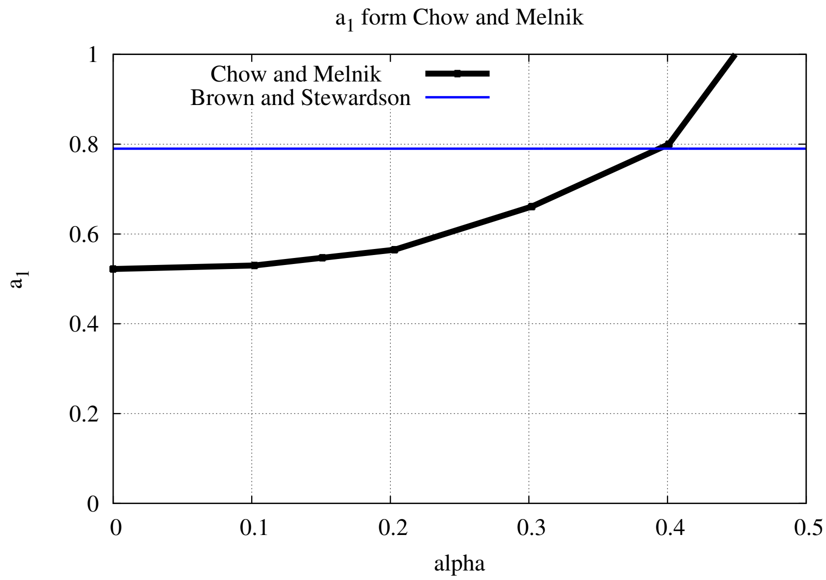

Figure 11: Variation of the parameter a_1 with (reduced) angle-of-attack from [4]. As a_1 approaches 0.47 this number diverges, indicating flow separation.

At the time when [42] appeared no computer codes for solving the set of equations Eqs. (39) to (43) were available. This occurred only in 1976 with the paper [4]. Instead of solving *Hilbert transform* Eq (40) directly Brown and Stewartson used some kind of an ad-hoc assumption concerning the pressure difference from the upper to the lower part around the TE as function of x which leads to the desired simplification and make the problem tractable analytically. The constant a_1 from 57 was analytically estimated to

$$a_1 = 2^{-1/2}\gamma^{-3/4}\cos\left(\frac{\pi}{8}\right) = 0.79 \qquad \text{with } \gamma = 3^{2/3}/\Gamma(1/3) = 0.7764\,. \tag{58}$$

$$\tag{59}$$

Later Chow and Melnik [4] improved the value for a_1 from a constant value (0.79) by Brown/Stewartson [42] to one dependent on the AOA, see Fig. 11. Thereby, separation is predicted for AOAs larger than $\alpha_S > 0.47$, which - in degrees - corresponds to rather small values of 3.8° for $RN = 10^5$. Quoting Crighton [44] this approach therefore

> provides detailed analytical and computational **understanding**,

(emphasis by the present author) as it gives a much less singular transition from the flat plate boundary layer $\sim RN^{-1/2}$ to Goldstein's wake $\sim RN^{-1/2} \cdot x^{1/3}$ already visualized in Fig. 9.

Preprints (www.preprints.org) | NOT PEER-REVIEWED | Posted: 9 November 2021 doi:10.20944/preprints202105.0496.v2

4.8 Turbulent Boundary Layers

The restriction of laminar boundary layers certainly forbids applications for $RN > 5 \cdot 10^5$. Therefore it is tempting to try to apply methods from TDT to turbulent boundary layers. This has been first attempted by Melnik and Chow [43] and is further discussed in [45, 39]. As a result Cousteix and Mass [39] conclude that - because no overlapping layer (the famous logarithmic law of the wall) exist - a chosen turbulence model has to be restricted to those which *leads us to the desired result.* However, recently Scheichl et al. [46] presented a *Uniformly Valid Theory for Turbulent Separation* based on the method of asymptotic analysis and TDT. They applied their approach to flow around a cylinder at very high RN($> 10^6$) and found a location of the separation point in fair agreement to what is known from measurements. How far these findings may be applied to the more general airfoil TE problem remains open.

5 Xfoil

A well known open source *aerodynamic engineering* code calls Xfoil [47, 13]. It uses what may be called *viscous/in-viscid coupling - interactive boundary layer theory*. It enjoys great popularity, see Oezlam et al. [48] for a recent review of its use regarding a specific wind turbine blade profile, DU00-W-210. Lift data from that tool is also included in our own comparison, see Fig. 13.

6 Comparison with CFD

Accurate numerical integration of the full Navier-Stokes Equations have been performed independently by [49, 36]. We have prepared computational meshes for two cases:

- A flat plate of unit length aligned with the inflow
- A simple 2D aerodynamic profile of finite thickness (NACA0015)

As a solver we use ANSYS-FLUENT V18 and ICEM/CFD for mesh preparation.

6.1 Flat Plate of Finite Length

Fig. 12 shows the development of the wake at $y = 0$ for $x \geq 0$ from TST and full CFD. The deviation may be caused by a too small calculational area (10 chords only).

To have a more quantitative comparison of TDT we compared highly sensitive drag data either calculated from the above mentioned CFD-model or from

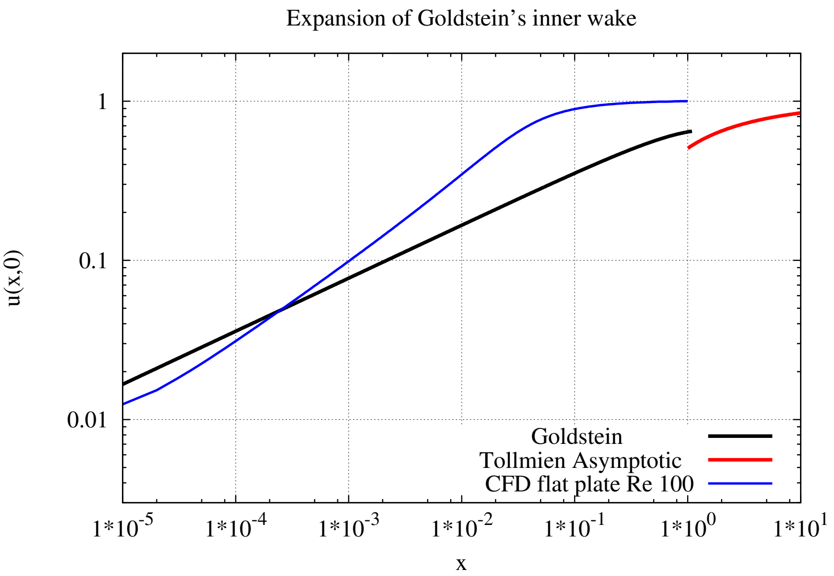

Figure 12: Center line velocity u(x,y=0) from Eq. (33) compared to a CFD model calculation. Note the double-logarithmic scaling of the axes and that the abscissa (scales according to TDT) covers 7 orders of magnitude. CFD profile reaches much earlier the asymptotic value, indicating a two small computational area.

 doi:10.20944/preprints202105.0496.v2

equations derived by TDT by different variants:

$$\text{Imai:} \quad c_D \sim \frac{1.33}{(RN \cdot x)^{1/2}} + \frac{2.32}{RN \cdot x} - \frac{2.20}{(RN \cdot x)^{3/2}} \log \sqrt{RN \cdot x} + \mathcal{O}(RN^{-3/2}) \,, \tag{60}$$

$$\text{Dean:} \quad c_D \sim \frac{1.33}{\sqrt{RN \cdot x}} + \frac{2.32}{RN \cdot x} + \mathcal{O}(RN^{-3/2}) \,. \tag{61}$$

as shown in table 1. Unfortunately, the contribution of the next-to-BL term

Table 1: Comparison of calculated flat plate drag data for various RN compared to CFD

RN	c_D	c_2	c_D Imai	c_D Dean
$1.23 \cdot 10^5$	$3.9 \cdot 10^{-3}$	3.04	$3.81 \cdot 10^{-3}$	$3.82 \cdot 10^{-3}$
$1.0 \cdot 10^4$	$1.43 \cdot 10^{-2}$	3.20	$1.34 \cdot 10^{-2}$	$1.35 \cdot 10^{-2}$
$1.0 \cdot 10^2$	$1.92 \cdot 10^{-1}$	3.31	$1.14 \cdot 10^{-1}$	$1.56 \cdot 10^{-1}$

$\sim RN^{-7/8}, c_2$ can only be compared at a 10% level. Even worse several hundreds of thousands of CFD-iterations have to be performed to be able to use a *Richardson*-type of extrapolation for the drag-coefficient. The meaning of this huge computational effort is clear: accurate CFD calculations to compare with accurate analytical theories demand computational resources that exceed usual turn-around times (in the order of minutes for 2D models) by a factor of more than 100. An example for RN=100: After $N_{iter} = 250$ k iterations drag force calculated by CFD was 0.1307, but an extrapolation to $N_{iter} \to \infty$ lowers this value by about 20% to 0.1174. Comparable findings were reported by McLachlan [36] and Dijkstra and Kuerten [50].

6.2 Thin Symmetric NACA Profile

As a last example to scrutinize the validity and accuracy of TDT we compare viscous correction from TDT with measurements for a 9%-thin NACA0009 airfoil, see Fig. 13. The measurements show some scatter but has been fitted to a simple three-parameter parabolic shape. As can be seen TDT (Eqs. (62) to (64)) describe the lowering of the lift-coefficient with some accuracy. It has to be noted that a somewhat thicker profile (NACA0012) has been investigated by Cebeci and Cousteix [51].

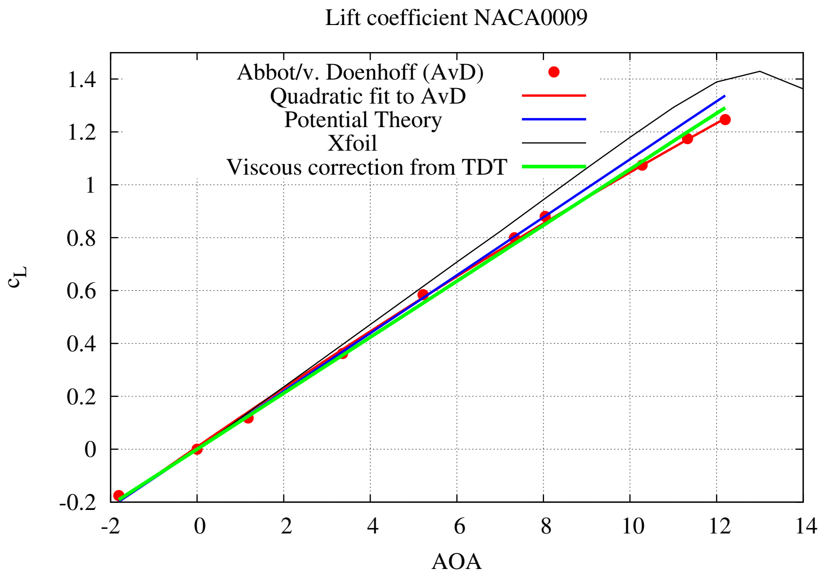

Figure 13: Lift coefficient of NACA0009 as function of angle of attack at RN = $6 \cdot 10^6$ together with potential theoretic prediction, data generated by Xfoil and viscous correction from TDT. Xfoil seems to predict a somewhat larger lift-slope which may be attributed to - as McLean [5]call it - the *fatness paradox*.

7 Summary and Conclusions

Within the Mathematical framework of matched asymptotic expansion, boundary layer theory can be extended to match Goldstein's wake to Blasius' flat plate boundary layer. With the use of $\epsilon = RN^{-1/8}$ as an expansion parameter Brown and Stewardson [42] were the first who presented a physical picture of the Kutta condition together with a quantitative viscous correction (in terms of a parameter B) for the slope of the lift coefficient:

$$\frac{c_L}{2\pi\alpha} = 1 - B \,, \quad (62)$$

$$B = a_1 \cdot \lambda^{-5/4}\epsilon^3 \,, \quad (63)$$

$$\text{with } 0.508 \le a_1 \le 1 \quad \text{for} \quad 0 \le \alpha \le \alpha_S(\approx 4^\circ) \,. \quad (64)$$

Therefore, the wake with its continuous pressure in y-direction enforces an equal continuous pressure for $y = 0$ across the trailing edge in x-direction and induces fixed (and finite) velocities, circulation and lift [38]. This can be formulated more precisely with reference to Fig. 10 discussing the behavior of the pressure around the trailing-edge in more detail:

The upper *near* TE flow outside the BL is higher than the lower one and as a consequence, the pressure above the trailing edge ought to be lower than the pressure immediately below. As a tendency for the flow in the near wake to be pushed upwards results. Introducing a Triple-Deck structure, the pressure behaves very differently: Even though upstream of the trailing edge, the pressure on the upper surface is lower than that on the lower surface, in the wake immediately after the trailing edge, TDT therefore will predict a reverse, that is the pressure in the wake for $y > 0$ will be higher than the pressure in the wake for $y < 0$ and so stabilize and maintain the flow leaving the trailing edge tangentially.

The following list is intended to summarize this logical sequence of arguments succinctly:

- The simplest model of a lift generating surface consists of a flat plate of finite length at a non-zero angle of attack.
- A Kutta-Joukovsky condition fixes circulation and thereby lift.
- Stated mathematically, it demands a finite velocity at the trailing edge.
- Matching Blasius' boundary layer with Goldstein's wake needs an additionally intermediate triple-structured layer of length of $RN^{-5/8}$ to interpolate between both different boundary conditions and avoiding singular behavior of the normal velocity component.
- Worked out, a set of equations results which predicts finite velocities and pressure around the trailing edge but a non-continuous pressure *gradient*.
- A viscous correction to the potential-theoretic lift coefficient slope of 2π can be derived and compared to experimental data.

- Extension to turbulent boundary layers is possible but still relies on the closure models.

8 Acknowledgments

Extended, intensive and very stimulating discussions with I.J. Sobey, University of Oxford, Oxford, UK and S. Braun, The Technical University of Vienna, Vienna, Austria during preparation of the manuscript are gratefully acknowledged. Gijs van Kuik, Delft Technical University, Delft, The Netherlands helped in reviewing later version of this paper, as Dr. Wang Zhongxia did with a later version. Brandon Lobo, Kiel University of Applied Sciences prepared Fig. 6 and helped to improve the text. The authors wishes to thank the referees as well for their comments

9 Abbreviations

Table 2: The following abbreviations have been used in this manuscript

AOA	Angle of attack α
BLT	Boundary layer theory
BoCo	Boundary Condition
CFD	Computational Fluid Dynamics
oDeqs	ordinary Differential Equations
M	Million
Ma	Mach number
pDeqs	partial Differential Equations
RANS	Reynolds Averaged Navier Stokes (Equations)
RN	Reynolds Number
TAT	Thin Airfoil Theory
TDT	Triple-Deck Theory
TE	Trailing Edge
c_L	Lift coefficient
c_D	Drag coefficient

Preprints (www.preprints.org) | NOT PEER-REVIEWED | Posted: 9 November 2021 doi:10.20944/preprints202105.0496.v2

10 Appendices

10.1 Decks and their Scales

The emergence of a two-folded boundary layer within the Goldstein wake (see Fig. 6) downstream of the TE including a singularity at least for the vertical velocity requires that there must be some kind of an additional transitional region around the TE, if one demands a smooth change of **all** variables. Using very different approaches, several papers and books, see, for example [52, 40, 39, 22], derive by carefully balancing inertial, viscous and pressure terms a set of algebraic equations for to define a structure which consists of

- a main part (or deck) of the boundary layer vertical size scales with $RN^{(-5/8)}$,
- below of that a smaller part (of height $RN^{(1/8)}$) which obeys classical BL type equations but with different BoCos (inner or lower deck) and finally
- an upper (or outer) part (deck) which carries the pressure distribution of vertical extension $RN^{(1/8)}$.

As already mentioned in section 4.5 the longitudinal (horizontal) scale of this triple structured region is $RN^{(-3/8)}$ which is $RN^{(1/8)}$ larger than the BL height as can be seen in Fig. 8.

10.2 Solution of the Upper Deck Equations

Equipped with these length-scales the expansion within the upper deck reads

$$u = 1 + \epsilon^{1/2} U_1^\star, \tag{65}$$
$$v = \epsilon^{1/2} V_1^\star, \tag{66}$$
$$v = \epsilon^{1/2} P_1^\star. \tag{67}$$

Mass conservation then reads (as it must)

$$U_{1,X}^\star + V_{1,X}^\star = 0 \tag{68}$$

Writing down the momentum-equation [53] gives a set of two linear but coupled pDEQs:

$$U_{1,X}^\star = -P_{1,X}^\star \tag{69}$$
$$V_{1,X}^\star = -P_{1,Y}^\star \tag{70}$$

As usual they have to be complemented by suitable (matching) BoCos from the *main*deck:

$$u = F_0(Y)' + \epsilon^{1/4} U_1, \quad (71)$$
$$v = \epsilon^{1/2} V_1, \quad (72)$$
$$v = \epsilon^{1/2} P_1, \quad (73)$$
$$\lim_{Y \to \infty} V_a(X,Y) = V_1^{\star}(X,0), \quad (74)$$
$$V_1^{\star}(X,0) = -{A_1}' \,. \quad (75)$$

Here $A_1(X)$ as already introduced in Eq. (38) appears as an *integration constant* of the equations of the *middle deck*:

$$U_{1,X} + V_{1,X} = 0, \quad (76)$$
$${F_0}' \cdot U_{1,X} + V_1 \cdot {F_0}'' \,. \quad (77)$$

Namely

$$U_1 = A_1(X) \cdot {F_0}''(Y), \quad (78)$$
$$V_1 = -{A_1}'(X) \cdot {F_0}'(Y) \,. \quad (79)$$

The solution process for Eq. (70) now works as follows [39]:

- Combine Eq. (70) with Eq. (76) to derive a Laplace equation for the pressure.
- Use the 2nd equation together with the last one of Eq. (75)
- Introduce Fourier transform with regard to X

$$P(\omega) = \frac{1}{\sqrt{2\pi}} \int P(X) e^{i\omega X} \, dX \quad (80)$$

- and finally perform Fourier Inversion to receive at:

$$P(X) = -\frac{1}{\pi} \int_{-\infty}^{\infty} \frac{A_1'(\zeta)}{X - \zeta} d\zeta \,, \quad (81)$$

A_1 already introduced in Eq. (40).

It is interesting to note that the above derived equation for the pressure disturbances resembles very much to integral expressions occurring in linearized aerodynamics or thin airfoil theory, see section (2.2).

10.3 Analytical Solution of a linearized Triple-Deck Model for Super-Sonic Flow

The sub-sonic case, described by the sets of equations Eqs. (39 to (43) - in general - can only be solved numerically. To gain more insight into the physics a more analytical solvable example is highly desirable. This model, valid for supersonic flow ($Ma > 1$ only) was provided in two papers of Stewartson & Williams [54, 55] and summarized in [2]. A major simplification (replacing the Hilbert transform relating pressure and displacement function) occurs when changing to compressible and hyper-sonic ($Ma_\infty > 1$)flow. Now the TDT equations read as:

$$p_2(X) = -A_1'(X) \; , \tag{82}$$
$$u_X + v_Y = 0 \; , \tag{83}$$
$$u \cdot u_X + v \cdot u_Y = A_1''(X) + u_{YY} \; , \tag{84}$$
$$\text{together with BoCos:} \tag{85}$$
$$u = v = 0 \text{ on } Y = 0 \; , \tag{86}$$
$$u \to Y \text{ as } X \to -\infty \; , \tag{87}$$
$$u \to Y + A_1(X) \text{ as } Y \to \infty \; . \tag{88}$$

Using an *Ansatz*

$$A_1(X) \sim -a_1 e^{cX} \; , \tag{89}$$
$$u \sim Y - a_1 e^{cX} f'(Y) \; , \tag{90}$$
$$v \sim c a_1 e^{cX} f(Y) \; , \tag{91}$$

an Airy type of DEQ ($f'' + Y \cdot f = 0$) follows with solution:

$$f(Y) = -\frac{c^{5/3}}{Ai'(0)} \int_0^Y \int_0^s Ai(c^{1/3 \cdot t}) \, dt \, ds \tag{92}$$
$$\text{with } c = \left(\frac{-Ai'(0)}{\int_0^\infty Ai(t) dt} \right)^{3/4} = 0.8272 \; . \tag{93}$$

[55] found as a solution for the wall shear stress

$$u_Y(X, Y = 0) \sim 1. - 1.91 \cdot e^{cX} \tag{94}$$

Fig 14 presents a comparison of the simple analytical solution, Eqs (82) to (88)and a full numerical solution gained with Sobey's code *sw.f* [2]. It shows that results from leading first order are able to show that *self induced separation occurs*, but numerical accuracy is poor. It has to be noted that the original paper [54] used a higher order Ansatz

$$u = Y - \sum_{n=1}^{\infty} e^{ncX} f'_n(Y), \tag{95}$$
$$v = \sum_{n=1}^{\infty} nce^{ncX} f_n(Y), \tag{96}$$
$$p = \sum_{n=1}^{\infty} a_n e^{ncX} \; . \tag{97}$$

Preprints (www.preprints.org) | NOT PEER-REVIEWED | Posted: 9 November 2021 doi:10.20944/preprints202105.0496.v2

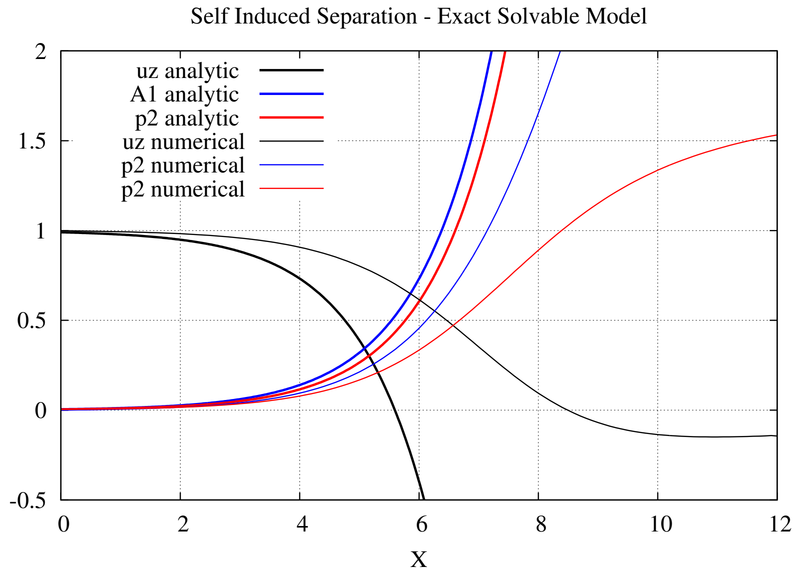

Figure 14: Comparison of wall shear stress, pressure and displacement function from leading order linearized TD approach and full numerical integration of boundary layer equation, Eqs. (82) to (88) with help of the code *sw.f* by [2]
.

 doi:10.20944/preprints202105.0496.v2

This resulted in three coupled DEqs, but the authors preferred to use a direct numerical integration of Eq. (83).

References

[1] Regis E. The Enigma of Aerodynamic Lift. SciAm. 2020;322(2):44 – 51.

[2] Sobey IJ. Introduction to Interactive Boundary Layer Theory. Oxford University Press, Oxford, UK; 2000.

[3] Van Dyke M. Perturbation Methods in Fluid Mechanics. The Parabolic Press, Stanford, CA, USA; 1975.

[4] Chow, R and Melnik, R E. Numerical Solution of the Triple-Deck Equations for Laminar Trailing-Edge Stall. In: Proc. 5th International Conference on Numerical Methods in Fluid Dynamics; 1976. p. 135–144.

[5] McLean D. Understanding Aerodynamics Arguing from the Real Physics. Wiley; 2013.

[6] van Kuik G. The Fluid Dyanmic Basis for Actuator Disc and Rotor Theories. IOS Press BV, Amsterdam, The Netherlands; 2018.

[7] Landau L, Lifshitz EM. Fluid Mechanics, 2nd Edition. Pergamon Press; 1987.

[8] McLean D. Aerodynamic lift, Part 1: The science. Phys Teach. 2018;56:516 – 520.

[9] McLean D. Aerodynamic lift, Part 2: Comprehensive Physical Explanation. Phys Teach. 2018;56:521 – 524.

[10] Bloor D. The enigma of the aerofoil. University of Chicago Press; 2011.

[11] Batchelor GK. An Introduction to Fluid Dynamics. Cambridge University Press; 1967.

[12] L Howarth. The Theoretical Determination of the Lift Coefficient for a Thin Elliptic Cylinder. Proc Roy Soc A. 1935;149:558–586.

[13] M Drela. XFOIL: An Analysis and Design System for Low Reynolds Number Analysis. Springer Notes in Engineering. 1989;54:1267–1289.

[14] W R Sears. Some Recent Developments in Airfoil Theory. J Aeor Sci. 1956;23, 5:490–499.

[15] J Y Zhu and T S Liu and L Liu and S F Zhou and J Z Wu. Causal mechanism in airfoil-circulation formation. Phys Fluids. 2015;27.

[16] Jeizhi Wu, Luoqin Liu and Tianshu Liu. Fundamental theories of aerodynamic force inviscous and compressible complex flows. Proc Aero Sci. 2018;99:27 – 63.

[17] Jones TD. Wing Theory. Princeton University Press; 1990.

[18] Freudenreich K, Kaiser K, Schaffarczyk AP, Winkler H, Stahl B. Reynnolds Number and Roughness Effects of Thick Airfoils for Wind Turbines. Wind Engineering. 2004;28(5).

[19] Yates JE. A Unified Viscous Theory of Lift and Drag of 2-D Thin Airfoils and 3-D Thin Wings. NASA; 1991. CR-4414.

[20] L W Bryant and D H Williams. An Investigation of the Flow of Air Around an Aërofoil of Infinite Span. Phil Tran Roy Soc A. 1926;225:626–635.

[21] S F Shen and P Crimi. The theory for an oscillating thin airfoil as derived from the Oseen equations. J Fluid Mech. 1965;23:585–609.

[22] Schlichting(deceased) H, Gersten K. Boundary Layer Theory, 9th Ed. Springer; 2017.

[23] Tianshu Liu, Shizhao Wang and Guowei He. Explicit Role of Viscosity in Generating Lift. AIAA JOURNAL. 2017;55, 11:3990 – 3994.

[24] Yates JE. Viscous Thin Airfoil Theory. Aeronautical Research Associates of Princeton Inc.; 1980. 413.

[25] Abbott I, von Doenhoff A. Theory of wing sections: Including a summary of airfoil data. Dover; 1959.

[26] J E Yates. Viscous Thin Airfoil Theory and the Kutta Condition. In: AIAA 16th Aerospace Science Meeting; 1978. p. 78–152.

[27] S Schmitz. Finite Domain Viscous Correction to the Kutta-Joukowski Theorem in Incompressible Flow. AIAA J. 2014;52, 9:2079–2083.

[28] S Schmitz and J G Coder. Inviscid Circulatory-Pressure Field Derived from the Incompressible Navier-Stokes Equations. AIAA J. 2015;53, 1:33–41.

[29] Schmitz S. Aerodynamics of Wind Turbines. Wiley; 2020.

[30] Brown SN, Stewartson K. Wake Curvature and the Kutta Condition in Laminar Flow. Aero Quart. 1975;26,4:175 – 280.

[31] Prandtl L. Über Füssigkeitsbewegung bei sehr kleiner Reibung. In: B G Teubner G Leipzig, editor. Verh. III. Math.-Kongr., Heidelberg; 1905. p. 484 – 491.

[32] Blasius H. Grenzschichten in Flüssigkeiten mit kleiner Reibung. Z Math Phys. 1908;56,1:1–37.

[33] Weyl H. On the Differential Equations of the simplest Boundary-Layer Problems. Ann Math. 1942;2:381 – 407.

[34] Boyd JP. The Blasius Function in the Complex Plane. ExpMath. 1999;8/4:381 – 394.

[35] Boyd JP. The Blasius Function: Computations Before Computers, the Value of Tricks, Undergraduate Projects, and Open Research Problems. SIAM reviews. 2008;50/4:791–804.

[36] McLachlan RI. The boundary layer on a flat plate. Phys Fluids. 1991;A 3(2):341 – 348.

[37] Goldstein S. Concerning some Solutions of the Boundary Layer Equations in Hydrodynamics. Proc Camb Phil Soc. 1930;XXVI,I.

[38] Sychev VV, Ruban AI, Sychev VV, Korolev GL. Asymptotic Theory of Separated Flows. Cambridge University Press, Cambridge, UK; 2008.

[39] Cousteix J, Mauss J. Asymptotic Analysis and Boundary Layers. Springer-Verlag Berlin Heidelberg; 2007.

[40] kam Yip KM. Model Simplification by asymptotic order of magnitude reasoning. Artificial Intelligence. 1996;80:309 – 348.

[41] Braun S. Recent developments in the asymptotic theory of separated flows. Leverhulme lectures - lecture notes, Manchester, UK; 2006.

[42] Brown SN, Stewartson K. Trailing-edge stall. J Fluid Mech. 1970;42,3:561 – 584.

[43] Melnik, R E and Chow, R . Asymptotic Theory of Two-Dimensional Trailing-Edge Flow. NASA; 1975. SP-347.

[44] Crighton DG. The Kutta Condition in Unsteady Flow. Ann Rev Fluid Mech. 1985;17:411 – 445.

[45] Cousteix J, Mauss J. Rational Basis of the Interactive Boundary Layer Theory. In: Meier GEA, Sreenivasan K, editors. One Hundred Years of Boundary Layer Research; 2004. p. 29–38.

[46] Scheichl B, Kluwick A, Smith FT, Paton J. A Uniformly Valid Theory of Turbulent Separation. In: M Oberlack et al , editor. Progress in Turbulence and Wind Energy IV; 2012. p. 85 – 88.

[47] Drela M. Flight Vehicle Aerodynamics. The MIT Press; 2014.

[48] Özlem, C Y and Pires, O and Munduate, X and Sørensen N and Reichstein, T and Schaffarczyk, A P and Diakakis, K and Papadakis, G and Daniele, E and Schwarz, M and Lutz, T and Prieto, R . Summary of the Blind Test Campaign to predict High Reynolds number performance of DU00-W-210 airfoil. AIAA 2017-0915. 2017;915.

[49] nd V C Patel HCC. Laminar Flow at the Trailing Edge of a Flat Plate. AIAA Journal. 1987;25(7):920 – 928.

 doi:10.20944/preprints202105.0496.v2

[50] Dijkstra, D and Kuerten, J G M. Asymptotics and Numerics for Laminar Flow over a Finite Flat Plate. In: Kaper, H G and Garbey, M , editor. Asymptotic and Numerical Methods for Partial Differential Equations with Critical Parameters; 1993. p. 135–144.

[51] Cebeci T, Cousteix J. Modeling and Computation of Boundary-Layer Flows. Horizons Publishing and Springer-Verlag Berlin Heidelberg; 1999.

[52] Nayfeh AH. Triple-Deck Structure. Computers Fluids. 1991;20(3):269 – 292.

[53] A P Rothmayer and F T Smith. 23 Incompressible Triple-Deck Theory. In: The Handbook of fluid dynamics. CRC Press and Springer-Verlag; 1998. .

[54] K Stewartson and P Williams. Self induced separation. Proc Roy Soc A. 1969;312:181 – 206.

[55] K Stewartson and P Williams. Self induced separation II. Mathematika. 1973;20(1):98 – 108.